Nonlinear Finite Element Modeling For High Strength Fibrous Reinforced Concrete Beams

Jaza Hassan Muhammad[1] - Asst lecturer
Dr. Mohamed Rauof Abdulkadir[1] - Professor
[1]Department of Civil Engineering – College of Engineering - University of Sulaimani

Received : 16/06/2016
Accepted : 09/10/2016
DOI Link: https://doi.org/10.17656/sjes.10043

Abstract

This paper presents a nonlinear finite element model to investigate the influence of steel fibers on the flexural strength of high strength reinforced concrete beams. Two methods had been used to model the steel fiber using ANSYS 14. In the first model the effect of steel fiber on the mechanical properties of concrete has been neglected, and the steel fiber considered as smeared reinforcement. In the second model the effect of steel fiber on the mechanical properties of concrete is considered in material modeling. The theoretical results were compared with the experimental result. And the variable present in both models was fiber volume fraction (0.00, 0.75, and 1.5) %. The experimental beams consist of high strength steel fiber reinforced concrete rectangular beams with sectional dimension (150 x 100) mm and overall length (3000) mm simply supported, and loaded through two points loading, those beams are used for verification of the proposed models.

Results showed that the first model is more reliable and compatible with experimental results than the second model. The analytical models also showed that increase in volume fraction of steel fiber improves the flexural rigidity and flexural strength of the high-strength fiber reinforced concrete beams.

Key words: high strength concrete, reinforced concrete beams, ANSYS 14, steel fiber, deflection.

1. Introduction

The term "high strength concrete" (HSC) is referred to concrete which has a compressive strength higher than 55MPa [1]. The use of high strength concrete in the construction industry has rapidly increased over the past years, which allow to design of smaller sections. Reducing the dead weight permits longer spans and more usable area of buildings. Reduction in mass is also important for economical design of earthquake resistance structures.

Reduction in member size means reducing stiffness that may create the serviceability problem of excessive deflection in flexural member. Therefore, it is important to check and control deflections of HSC members under service loads [2]. High-strength concrete is also a brittle material, and as the concrete strength increases the post-peak portion of the stress-strain diagram descends steeply. The reduced stiffness and lack of ductility is a serious drawback for the use of high-strength concrete, because the maximum potentiality of high-strength concrete cannot be realized fully in structures [3]. The compromise between the previous inverse characteristics of concrete can be obtained by adding discontinuous fibers [3].

Al Ta'an et al [4] proposed a nonlinear three dimensional finite element model for steel fiber reinforced concrete deep beam considering the effect of steel fiber on the material properties of concrete only.

Islam et al [5] proposed a finite element model, to investigate the flexural capacity of RC beams made of steel fiber reinforced concrete, however

they also considered the effect of steel fiber on the material properties of concrete only.
The aim of this paper is to carry out a finite element modeling for High Strength Steel Fiber Reinforced Concrete (HSSFRC) beams and studying the effect of steel fiber on the flexural strength and deformation characteristics of high strength concrete beam reinforced with conventional steel bars through the models proposed.

2. Research Significance

The investigation presents an analytical model using non linear finite element technique using ANSYS software to model the inclusion of steel fiber in high strength reinforced concrete beams. The study also aims to demonstrate analytically the effect of volume fraction of the steel fiber on flexural rigidity and flexural strength of the high-strength fiber reinforced concrete beams.

3. Methodology

Finite element analysis was carried out by using the ANSYS 14 program. ANSYS is capable of performing numerical models for the nonlinear behavior of concrete under static and dynamic loading. ANSYS was chosen because it has a wide range of elements and constitutive models for different materials including concrete. Two models were investigated as described below.

3.1. Model No. 1

In model-1, the effect of steel fiber on the mechanical properties of concrete is neglected, and the steel fiber is modeled as smeared reinforcement in ANSYS 14.

3.1.1. Elements

Element SOLID65 is used for the 3-D modeling of concrete with and without steel fiber. It is capable of cracking in tension and crushing in compression. The element is defined by eight nodes having three degrees of freedom at each node: translations in the nodal x, y, and z directions [6]. The most important aspect of this element is the treatment of nonlinear material properties. The concrete is capable of cracking in three orthogonal directions, crushing, and plastic deformation [7]. Rebars capable of tension and compression can be provided in this element. The geometry, node locations, and the coordinate system for geometry of element SOLID65 are shown in Figure 1.
Smeared reinforced method is used to model the steel fiber. In this method, the concrete and the reinforcing are discretized into elements with the same geometrical boundaries and the effects of reinforcing are averaged within the pertaining element [8].
Element LINK180 is a 3-D spar and can be used to model the deformed steel bar. The element is a uniaxial tension-compression element with three degrees of freedom at each node: translations in the nodal x, y, and z directions [6]. The element is defined by two nodes, the cross-sectional area and the material properties are also defined. The geometry, node locations, and the coordinate system for this element are shown in Figure 2.

3.1.2. Material modeling

Concrete: for first model the high strength concrete uniaxial compressive strength without the effect of steel fiber on the mechanical properties of concrete is used. The stress-strain curve adopted for concrete is linearly elastic up to about 30 percent of the maximum compressive strength [7] as shown in Figure 3, and the secant modulus of elasticity for high strength concrete is estimated by the equation 1 below.

$$E_c = 3320\sqrt{f'_c} + 6900 \quad \ldots\ldots\ldots (1)$$

After the elastic limit a multi-linear isotropic concrete model is used for the nonlinear part. The Von Mises failure criterion along with Willam and Warnke model is used to define the failure of concrete [6]. The compressive uniaxial stress-strain relationship for high strength concrete model shown in Figure 3 was obtained by using the equation 2 [9].

$$f_c = f'_c \left[\frac{\beta\left(\frac{\epsilon}{\epsilon_o}\right)}{\beta - 1 + \left(\frac{\epsilon}{\epsilon_o}\right)^{\beta k}} \right] \quad \ldots\ldots\ldots (2)$$

Where:
$\beta = 0.058f'_c + 0.8$
$\epsilon_\circ = \frac{f'_c}{E_c}\left(\frac{\beta}{\beta-1}\right)$
$k = 1 \qquad for \ \frac{\epsilon}{\epsilon_\circ} \le 1$
or
$k = 0.67 + \frac{f'_c}{62.05} \qquad for \ \frac{\epsilon}{\epsilon_\circ} > 1$

Cracking and crushing are determined by a failure surface. Once the failure surface growth, concrete crack occurs if any principal stress is tensile, while the crushing occurs if all principal stresses are compressive.

The failure surface for compressive stresses is based on Willam-Warnke failure criterion which depends on five material parameters. Tensile stress consists of a maximum tensile stress criterion: a tension cutoff. When the failure surface is reached, stresses in that direction have a sudden drop to zero, there is no strain softening neither in compression nor in tension [6]. Two shear transfer coefficients were used, one βt=0.3 for open cracks and the other for closed cracks βc=1, are used to consider the retention of shear stiffness in cracked concrete. Typical shear transfer coefficients range from 0.0 to 1.0, with 0.0 representing a smooth crack (complete loss of shear transfer) and 1.0 representing a rough crack (no loss of shear transfer)[6]. The uniaxial cracking stress is assumed equal to the modulus of rapture obtained by the equation 3 below.

$$f_r = 0.94\sqrt{f'_c} \quad \ldots\ldots\ldots\ldots\ldots\ldots (3)$$

Steel bar : The stress-strain curve shown in Figure 4 is adopted for the steel bars. Steel reinforcement behavior is linear elastic prior to initial yield, the initial yield is followed by a yield plateau then strain hardening begins until failure occurs. Table.1 shows the Elastic properties of the steel bar used in the model. After the yield plateau the inelastic range is represented by multi-linear isotropic model. The Von Mises failure criterion is used. The stress-strain curve of steel bar was modeled by Sargin[11] and shown by equation 4.

$$f_s = E_s\epsilon_s \qquad for \quad 0 \le \epsilon_s \le \epsilon_y$$
$$f_s = f_y \qquad for \quad \epsilon_y \le \epsilon_s \le \epsilon_{sh}$$
$$f_s = f_y + E_{sh}(\epsilon_s - \epsilon_{sh})\left[1 - \frac{E_s(\epsilon_s - \epsilon_{sh})}{4(f_{su} - f_y)}\right]$$
$$for \ \epsilon_s > \epsilon_{sh} \quad \ldots\ldots\ldots\ldots\ldots\ldots (4)$$

f_{su} =620MPa , E_{sh}= 6900 MPa and ϵ_{sh}=0.0075 mm/mm

Steel fiber: The material model for steel fiber adopted is linear elastic prior to initial yield, beyond the initial yield it is perfectly plastic in tension and compression loading as shown in Figure 5. After the elastic limit the inelastic bilinear isotropic model is adopted and the Von Mises failure criterion is used. The stress-strain curve of steel fiber modeling is as follows [12]:

$$\sigma_{fu} = 2\tau\left(\frac{L_f}{d_f}\right) \ldots\ldots\ldots\ldots\ldots\ldots (5)$$

$$L_c = \frac{\sigma_y\, d_f}{2\tau}$$

$$\eta_l = \begin{cases} \frac{L_f}{2L_c} & L_f \le L_c \\ 1 - \frac{L_c}{2L_f} & L_f \ge L_c \end{cases}$$

$$\sigma_f = \eta_l \sigma_{fu} \quad \ldots\ldots\ldots\ldots\ldots\ldots (6)$$

3.2. Model No. 2

In model-2, contribution of the effect of steel fiber on the mechanical properties of the concrete is considered in material modeling in the ANSYS 14.

3.2.1. Elements

The same elements that were used in Model-1 as described above (SOLID 65 for concrete and LINK180 for steel bar) are used for Model-2.

3.2.2. Material modeling

Steel fibrous Concrete : for Model-2 the uniaxial compressive strength of the High Strength Steel Fibrous Concrete is used. As shown in Figure 6 and Figure 7 the stress-strain curve for High Strength Steel Fiber Concrete, for two different steel fiber volume fractions is linearly elastic before the start of the curved part.

After the elastic limit the inelastic is modeled as multi-linear isotropic concrete model. The Von Mises failure criterion along with Willam and Warnke model is used to define the failure of concrete. The compressive uniaxial stress-strain relationship for high strength steel fiber concrete model, shown in figure 6 and figure 7 was obtained by using the equation 7 [13].

$$f_c = f'_{cf}\left[\frac{\beta\left(\frac{\epsilon}{\epsilon_\circ}\right)}{\beta-1+\left(\frac{\epsilon}{\epsilon_\circ}\right)^{\beta}}\right] \ldots\ldots\ldots\ldots\ldots (7)$$

Where:

$$E_{it} = (10300 - 400V_f)(f'_c)^{1/3}$$

$$\epsilon_\circ = \left[0.0005 + 0.00000072\left(\frac{V_f l_f}{d_f}\right)\right](f'_c)^{0.35}$$

$$\beta = \frac{1}{1 - \frac{f'_c}{\epsilon_\circ E_{it}}}$$

The same two shear transfer coefficients used for model-1 are also used in model-2

3.3. Verification of the proposed Models

The experimental tests carried out by Ashor et al [14] were modeled by the proposed methods to verify the proposed models.

The beams are shown in Figure 8 they were singly reinforced with a flexural tensile reinforcement of 2ϕ10mm. Three volume fractions of steel fibers V_f (0.0, 0.75 and 1.5) percent were used.

The compressive strength of the high strength concrete without fiber was 80.19 MPa and the elastic properties of the concrete are shown in Table 2. The beams designation and steel fiber volume fraction and concrete cracking and compressive (crushing) strength are given in Table 3. The properties of the steel fiber are shown in Table 4.

The volume of steel fiber, which is in the direction of longitudinal axis of beams was determined by multiplying the volume fraction of steel fiber with the orientation factor $\eta_\circ$ =0.41[15]

4. Results and discussion

Figures (9, 10, and 11) show the mid span load-deflection relationship for the tested and modeled beams for various steel fiber volume fraction ratios, where BE represents the experimental test beams and B1 and B2 the modeled beams model-1 and model-2 respectively. Table 5 also shows the mid-span deflection values at load of 15 kN for the tested beams and their ANSYS models (1) and (2). All the three figures and Table5 show that the comparison between the experimental results and analysis model-1 results are very comparable and well related, however results from ANSYS model-2 are very different, except for the beam BE-0 without steel fibers where the ratio is 1.07. These results indicate that high strength fiber reinforced concrete beam can be analyzed for its behavior under flexural loading using ANSYS model-1.

The effect of the inclusion of steel fibers is clearly indicated by the analysis model-1 as shown in Figure 12. The addition of steel fibers has reduced the deflection values at the same load level and has enhanced the toughness and ductility of the beams in bending. However in analysis model-2 the deflection is not affected significantly but ductility enhancement is also apparent as shown in Figure 13.

Figure 14 shows the crack patterns of the beams in both models. The length of cracks in Model-1 is lesser than the length of cracks in model-2 for a specific load. This indicates that the effective moment of inertia of model-1 is greater than the effective moment of inertia of model-2 for any specific load, consequently less deflection as observed in the Figures 10 and11.

The effect of volume fraction of steel fibers on load-deflection relationship for high strength reinforced concrete beams appears after the appearance of the first crack. Using the volume fraction of 0.75 and 1.5 percent reduces the deflection at any loading, for example in model-1 analysis at load of 15 kN, the deflection at mid span of the non-fibrous high strength concrete beam is 66.38 mm, however for HS fibrous beams mid span deflection at the same load are 26.82 mm and 17.64 mm for beams with volume fractions of 0.75% and 1.5% respectively. The same pattern is true for analysis model-2 with less accuracy . The ratios of analysis deflection results to experimental deflections are much higher because near ultimate the deflection is over estimated by the analysis due to the assumptions made in model-2, the cracks near ultimate propagate more in the compression region as shown in Figure 14, consequently producing higher deflection.

The failure load for the tested beams is also affected by the inclusion of steel fibers as seen in Table 6. The table shows the failure load due to steel reinforcement yielding in both the experimental beams and the model-1 beams for the three steel fiber volume fractions (0.0, 0.75%, and 1.5%). The values of the experimental and the analysis failure loads are close and comparable. The failure load enhancement due to inclusion of steel fibers are 17.45% and 37.01% for the experimental tested beams and the increases are 15.38% and 23.08% for the same beams in model-1 analysis for steel fiber volume fractions of 0.75% and 1.5% respectively. This indicates a close comparison of results for failure loads as well.

5. Conclusion

From the results obtained in this study the following conclusion can be drawn:

1- The proposed theoretical model-1 for the analysis of High Strength Fibrous Reinforced Concrete Beams by using ANSYS14 modeling the steel fiber as smeared reinforcement is an appropriate model to simulate the behavior of HSFRCB.
2- Using this analytical model it was observed that by adding steel fiber to High strength reinforced concrete beams, the load carrying capacity of the beams after the first crack increased and the deflection was decreased.
3- The analytical model-1 demonstrates well the cracking pattern and load-deflection behavior of the tested beams.
4- Addition of steel fibers to high strength reinforced concrete beams increased the ductility of the beams in flexure; this was clearly demonstrated by both analytical models

Notation

d_f Fiber diameter, mm
E_{it} Initial tangent modulus, MPa
E_c Modulus of elasticity of HSC, MPa
E_s Modulus of elasticity of steel bar, MPa
E_{sh} Tangent modulus at initial strain hardening of steel bar, MPa
f'_c Cylinder compressive strength of plain concrete, MPa
f_c Concrete stress at any strain, MPa
f_{cf} Cylinder compressive strength of fiber reinforced concrete, MPa
fr Modulus of rupture of concrete , MPa
f_y Yield stress of reinforced steel bar, MPa
f_s Steel stress at any strain, MPa
k Factor to control the slops of the ascending and descending branches of the stress-strain curve
l_f Fiber length, mm
Lc Critical fiber length, mm. i.e. twice the length of fiber embedment which would cause fiber failure in a pull-out test
V_f Volume fraction of steel fiber, %
ϵ_o Concrete strain at peak stress
ϵ Concrete strain
ϵ_s Strain in steel bar
ϵ_{sh} Strain at onset of strain hardening
ϵ_{su} Strain at peak stress in steel bar
β A curve fitting factor
τ Interfacial bond between fiber and concre
σ_{fu} Maximum failure stress of fully bonded fibers, or pullout stress of debonded fibers
η_l Efficiency factor for fiber length
η_o Efficiency factor for fiber orientation=0.41

References

1- ACI Committee 363, "State of the Art Report on High-Strength Concrete", ACI 363R-10, American Concrete Institute, Detroit, 2010, p.3.
2- Ashour S. A., Mahmood K. and Wafa F. F., "Influence of Steel Fibers and Compression Reinforcement on Deflection of High Strength Concrete Beams", ACI Materials Journal V.94, No. 6, November-December 1997, pp. 611-624
3- Wafa, F. F. and Ashour, S. A., "Mechanical Properties of High- Strength Fiber Reinforced Concrete", ACI Materials Journal, V. 89, No. 5, September-October 1992, pp. 449-455.
4- Al-Ta'an S. A., Mohammad A. A. and Al-Jurmaa M. A. "nonlinear three dimensional finite element analysis of steel fiber reinforced concrete deep beam",The Iraqi Journal for Mechanical and Materials Engineering,2010,pp. 13-25
5- Islam M. M. and et al "finite element modeling, analysis and validation of the flexural capacity of RC beams made of steel fiber reinforced concrete (SFRC) ",2nd International Conference on Advances in Civil Engineering 26 –28 Dec, 2014 CUET,pp.540-547
6- ANSYS,Inc."Theory Reference for the Mechanical APDL and Mechanical Applications", ANSYS help, Release 9, April 2009, p.672.
7- Kachlakev D., Miller T., Yim S., Chansawat K and Potisuk T. "Finite Element Modeling of Reinforced Concrete Structures Strengthened with FRP Laminates",

SPR 316, Oregon Department of transportation – Research Group, May 2001,P.6.

8- Dahmani L., Khennane A. and Kaci S. "Crack Identification In Reinforced Concrete Beams Using ANSYS software", Strength of Materials, Vol. 42, No. 2, 2010, pp. 232-240.

9- Wight J. K. and MacGregor J. G. "Reinforced Concrete Mechanics and Design", Pearson Education, Fifth edition, 2009, pp.84.

10- Musmar M. A., Rjoub M. I. and Abdel Hadi M. A. "Nonlinear Finite Element Analysis of Shallow Reinforced Concrete Beams Using Solid65 Element", ARPN Journal of Engineering and Applied Sciences, VOL. 9, NO. 2, 2014, pp.85-89.

11- Sargin, M., "Stress-Strain Relationship for concrete and the Analysis of Structural Concrete Sections,". Study No. 4, Solid Mechanics Division, University of Waterloo, 1971, pp. 167.

12- Hannant, D. J., "Fiber Cement and Fiber Concrete", Wiley interscience publication, IBSN 0471996203, 1978, pp.12-27

13- Mansur M. A., Chin M. S. and Wee T. H. "Stress-strain Relationship of High-Strength Fiber Concrete in Compression", Journal of Materials in Civil Engineering, Vol. 11, No. 1, February 1999, pp.21-29.

14- Ashour S. A. and Wafa F. F. "Flexural Behavior of High-Strength Fiber Reinforced Concrete Beams", ACI Structural Journal, V.90, No. 3, May-June 1993, pp.279-287.

15- Romuald J. P. and Mandel J. A. "Tensile Strength of Concrete Affected by Uniformly Distributed and Closely Spaced Short Lengths of Wire Reinforcement", ACI Journal proceedings V. 61, No. 6 June 1964, pp. 657-671.

16- Swamy R. N., " The Interfacial Bond Stress in Steel Fiber Cement Composites", Cement and Concrete Research. Vol. 6, 1976, pp. 641-650.

إستخدام العناصر المحددة غير الخطية لتحليل العتبات الخرسانية المسلحة عالية المقاومة والمعززة بالألياف الفولاذية

جزا حسن محمد[1] – مدرس مساعد
د . محمد رؤوف عبدالقادر[1] – استاذ
[1] قسم الهندسة المدنية – جامعة السليمانية

المستخلص :
يقدم هذا البحث نموذجا للعناصر المحددة غير الخطية لدراسة تأثير الألياف الفولاذية على مقاومة الانثناء للعتبات الخرسانية المسلحة عالية المقاومة . وقد استخدم طريقتين لتمثيل الألياف الفولاذية باستعمال ANSYS14. في النموذج الأول تم إهمال تأثير الألياف الفولاذية على الخواص الميكانيكية للخرسانة وأعتبرت الألياف الفولاذية كتسليح داخل كل عنصر . في النموذج الثاني أخذت بنظر الأعتبار تأثير الألياف الفولاذية على الخواص الميكانيكية للخرسانة و ذلك عند تمثيل المواد . وتمت مقارنة النتائج النظرية مع النتائج المختبرية . وكان المتغير في كلا النموذجين نسبة المحتوى الحجمى للألياف . (1.5 ، 0.75 ، 0 %) . يتكون النموذج التجريبي من عتبة من الخرسانة المسلحة عالية المقاومة والمعززه بالألياف الفولاذية بأبعاد (150×100)ملم وطول كلى (3000)ملم بسيطة الأسناد.

أظهرت النتائج أن النموذج الأول أكثر توافقاً مع النتائج المختبرية مقارنة بالنموذج الثاني . كما بينت النتائج التحليلية أيضا أن الزيادة في نسبة حجم الألياف تحسن من صلابة الانثناء ومقاومتها في العتبات الخرسانية المسلحة عالية المقاومة والمعززة بالألياف الفولاذية.

الكلمات المفتاحية : الخرسانية عالية المقاومة ، العتبات الخرسانية المسلحة ، ANSYS 14 الألياف الفولاذية ، الانثناء .

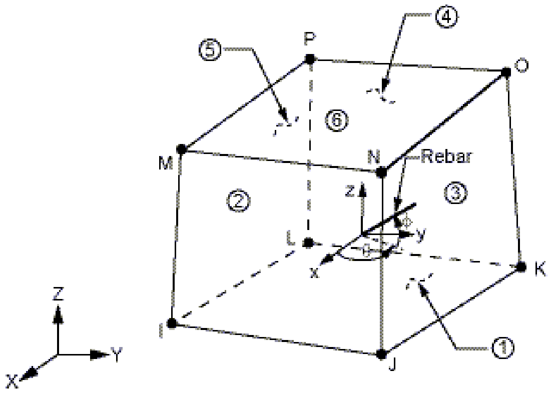

Fig. (1) : Solid65 geometry.

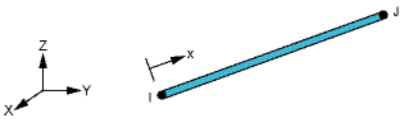

Fig. (2) : Link180 geometry.

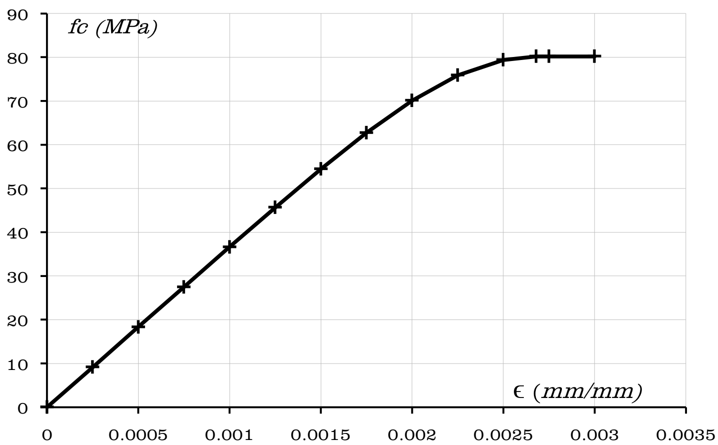

Fig. (3) : Stress-strain curve for high strength concrete.

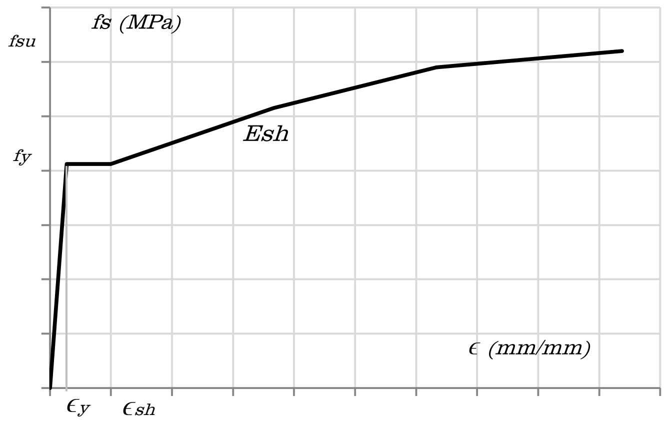

Fig. (4) : Stress-strain curve for steel bar.

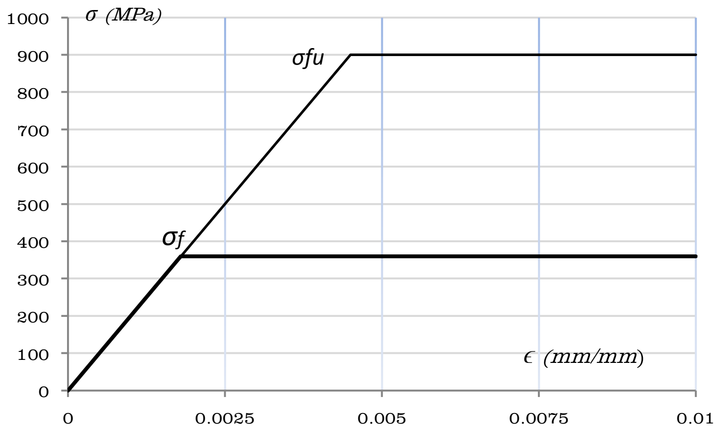

Fig. (5) : Stress-strain curve for steel fiber.

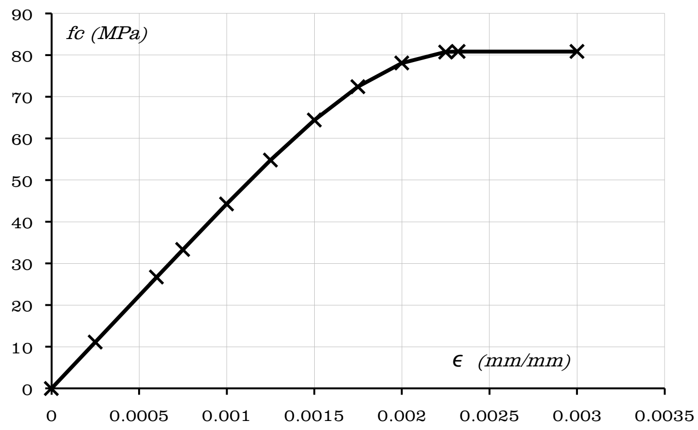

Fig. (6) : Stress-strain curve for high strength fibrous concrete (V_f = 0.75).

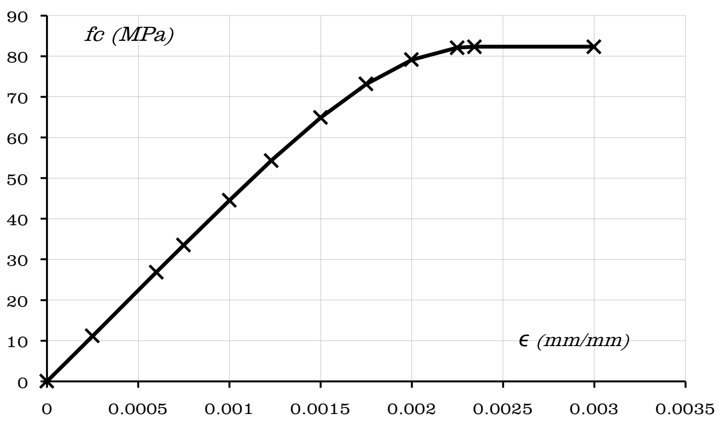

Fig. (7) : Stress-strain curve for high strength fibrous concrete (V_f = 1.5).

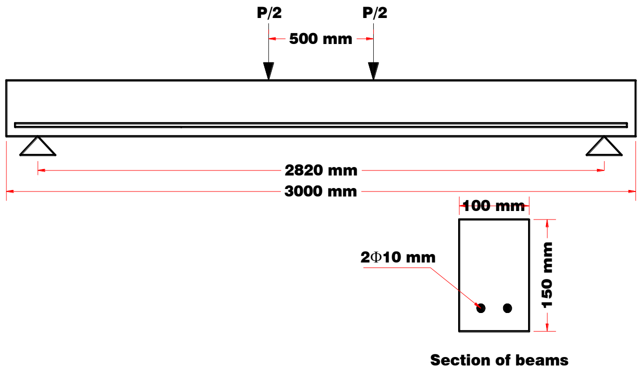

Fig. (8) : Dimension and reinforcement detail of tested beams with loading.

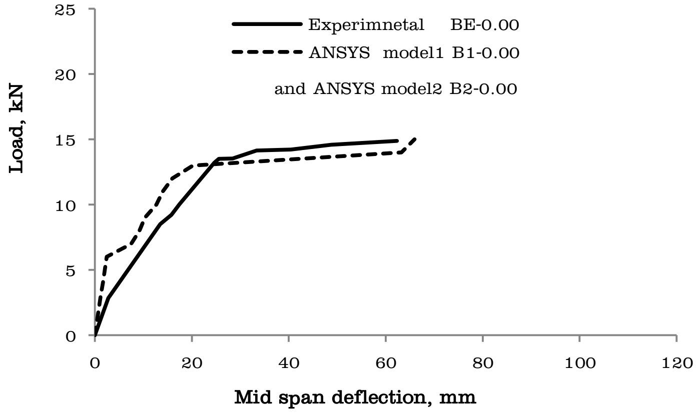

Fig. (9) : Load deflection relationship for beams with *Vf*=0.00

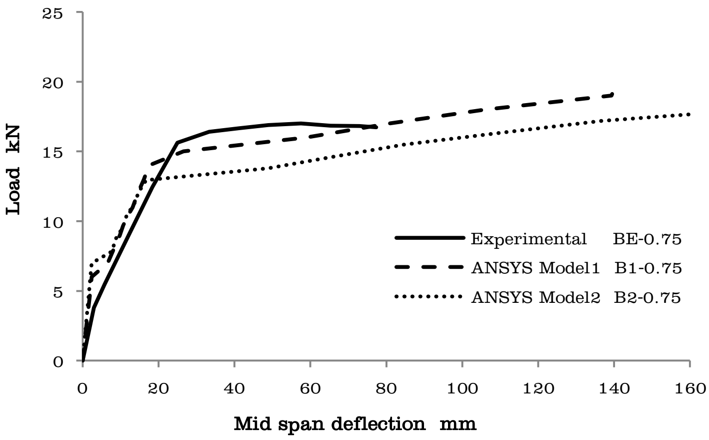

Fig. (10) : Load deflection relationship for beams with *Vf*=0.75.

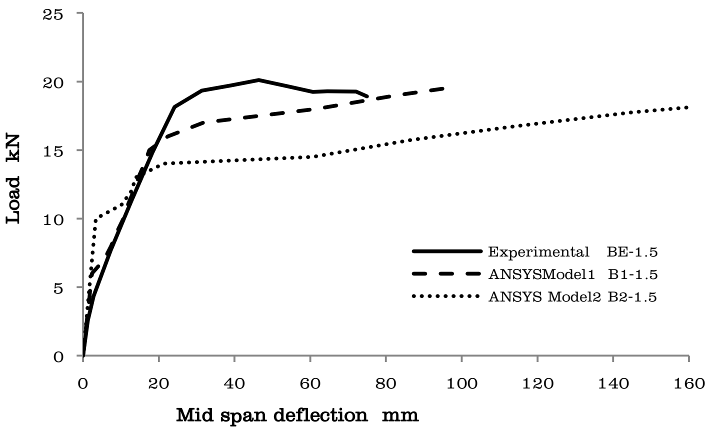

Fig. (11) : Load deflection relationship for beams with *Vf*=1.5.

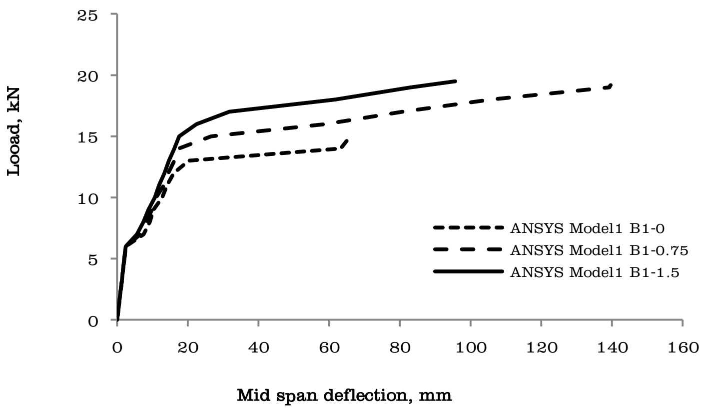

Fig. (12) : Load deflection relationships for various steel fiber content for model-1 analysis.

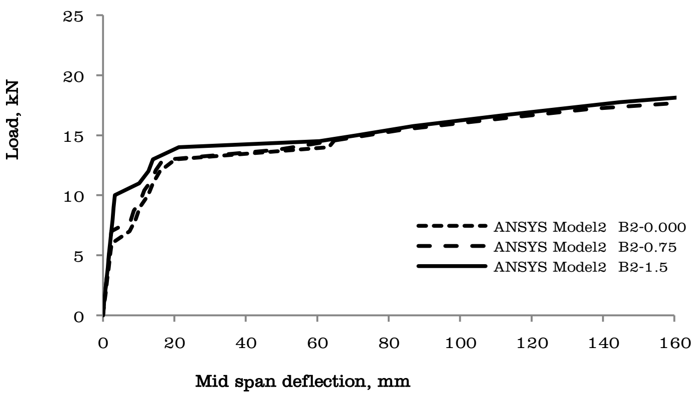

Fig. (13) : Load deflection relationships for various steel fiber content for model-2 analysis.

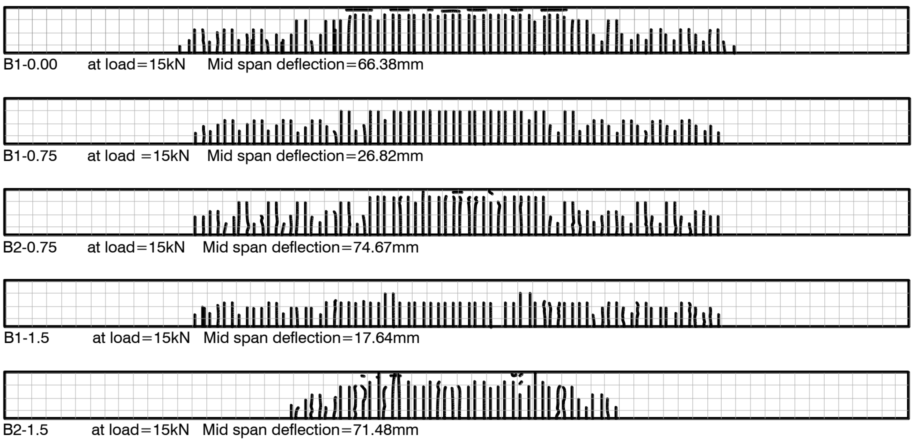

Fig. (14) : Crack pattren of the modelled beams.

Table (1) : Elastic properties of steel bar (Ref.7)

Material	Material model	Modulus of elasticity MPa	Poisson's ratio
Steel	Linear elastic isotropic	200000	0.3

Table (2) : Elastic properties of concrete.

Material	Material model	Modulus of elasticity MPa	Poisson's ratio
	Vf = 0.00		
concrete	Linear elastic isotropic	36640	0.2*
	Vf = 0.75		
Steel fibrous concrete	Linear elastic isotropic	44520	0.2
	Vf =1.5		
Steel fibrous concrete	Linear elastic isotropic	44760	0.2

** This value takes from reference No. 7*

Table (3) : Beam designation's for both Models

Beam designation	Fiber Volume fraction (%)	Compressive strength concrete MPa	Tensile strength of concrete MPa
BE-0.0	0	80.19	8.42
BE-0.75	0.75	80.87	9.04
BE-1.5	1.5	82.32	14.04

Table (4) : properties of steel fiber.

Material	Steel fiber
Length *Lf* (mm)	60
Diameter *df* (mm)	0.8
Yield stress of steel fiber, σy (MPa)	1130
interfacial bond, τ (Mpa)	6 [16]
Material model	Linear elastic isotropic
Modulus of elasticity Mpa	200000
Poisson's ratio	0.3[7]

Table (5) : Mid-span deflection for the tested beams and analysis models (1) and (2).

beams	Δ at load =15kN mm	Ratio analysis/exp
BE-0.00	62	
B1-0.00	66.38	1.07
B2-0.00	66.38	1.07
BE-0.75	24	
B1-0.75	26.82	1.11
B2-0.75	74.68	3.11
BE-1.5	18.3	
B1-1.5	17.64	0.96
B2-1.5	71.48	3.91

Table (6) : effect the volume fraction of steel fiber on yield load.

Beams	At yielding		
	Load kN	Increase %	Deflection mm
BE-0.00	13.24	-	24.46
BE-0.75	15.55	17.45	24.75
BE-1.5	18.14	37.01	23.76
B1-0.00	13	-	20.25
B1-0.75	15	15.38	25.81
B1-1.5	16	23.08	22.6